A&A manuscript no.
(will be inserted by hand later)

Your thesaurus codes are:

ASTRONOMY AND ASTROPHYSICS
October 31, 2000

XMM-Newton Observatory ⋆

I. The Spacecraft and Operations

F. Jansen[1], D. Lumb[1], B. Altieri[2], J. Clavel[2], M. Ehle[2], C. Erd[1], C. Gabriel[2], M. Guainazzi[2], P. Gondoin[1], R. Much[1], R. Munoz[2], M. Santos[2], N. Schartel[2], D. Texier[2], and G. Vacanti[1]

[1] Astrophysics Divn., Space Science Dept., ESTEC Postbus 299, Noordwijk 2200AG, Netherlands
[2] ESA Villafranca Satellite Tracking Station, Apartado 50727, E-28080 Madrid, Spain

Received September 30, 2000; accepted

Abstract. The XMM-Newton Observatory is a cornerstone mission of the European Space Agency's Horizon 2000 programme, and is the largest scientific satellite it has launched to date. This paper summarises the principal characteristics of the Observatory which are pertinent to scientific operations. The scientific results appearing in this issue have been enabled by the unprecedentedly large effective area of the three mirror modules, which are briefly described. The in-orbit performance and preliminary calibrations of the observatory are briefly summarised. The observations from the XMM-Newton calibration and performance verification phase, which are public and from which most papers in this issue have been derived, are listed. The flow of data from the spacecraft, through the ground segment, to the production of preliminary science products supplied to users is also discussed.

Key words: Instruments - X-ray astronomy

1. Introduction

On December 10, 1999 the XMM-Newton space observatory, was placed in a 48 hours orbit by the first commercial Ariane-V launch, V504. XMM-Newton is a cornerstone project in the ESA Horizon 2000 programme. Following an original proposal made to the agency in 1982, the primary objectives for the XMM-Newton mission were initially discussed by the scientific community at an ESA organised workshop, held in Lyngby, Denmark, in June 1985. High quality X-ray spectroscopy on faint sources was identified as the major next step following a series of X-ray missions flown in the 1990's. A key technology component to allow this advance was the development by ESA of the large area X-ray mirror modules. The measured in-orbit performance of these mirrors is described in section 2.1. The early in-orbit calibration status of the instrumentation was confirmed by comparisons with extensive ground-based activities.

Send offprint requests to: F. Jansen

⋆ Based on observations obtained with *XMM-Newton*, an ESA science mission with instruments and contributions directly funded by ESA Member States and the USA (NASA)

2. Spacecraft

The 4 tonne, 10m long XMM-Newton spacecraft is the largest scientific satellite ever to be launched by the European Space Agency. It comprises two large payload modules connected by a long carbon fibre tube which forms the telescope optical bench (Figure 1). On the Focal Plane Assembly are located the two Reflection Grating Spectrometer (den Herder, Brinkman and Kahn et al) readout cameras, an EPIC PN (Strüder, Briel and Dennerl et al) and two EPIC MOS imaging detectors (Turner, Abbey and Arnaud et al). The spacecraft Service Module contains most of the spacecraft sub-systems, as well as the Optical Monitor instrument (Mason, Breeveld and Much et al), star trackers and the three X-ray Mirror Modules.

2.1. The X-ray telescopes

Each of the three x-ray telescopes on board XMM-Newton consists of 58 Wolter I mirrors which are nested in a coaxial and confocal configuration (Aschenbach, Citterio and Ellwood et al). This design provides a large collecting area over a wide energy band. The mirror grazing incidence angles range between 17 and 42 arcmin. Their focal length is 7.5 meters and the diameter of the largest mirrors is 70 cm, to be compatible with the shroud of the launcher.

Mirrors were replicated from superpolished gold coated mandrels using a nickel electroforming technique (Gondoin et al 1994). The 58 mirrors of each telescope are bonded on their entrance aperture to the 16 spokes of a single spider. An electron deflector is located in the exit aperture. It produces a circumferential magnetic field which prevents low energy electrons reflected by the mirrors reaching the focal plane detectors. X-ray baffles consisting of two sieve plates each with 58 annular apertures

Table 1. Specifications of an XMM−Newton telescope

telescope focal length	7500 mm
number of mirrors per telescope	58
outer mirror radius	350 mm
inner mirror radius	153 mm
axial mirror length	600 mm
outer mirror thickness	1.07 mm
inner mirror thickness	0.47 mm
minimum packing distance	1 mm
mirror substrate material	Nickel
reflective coating	Gold

are located in front of the mirror systems. They act as collimators and considerably reduce the amount of straylight in the field of view of the focal plane cameras.

The point spread functions and effective areas of the telescopes were first characterized on-ground during an extensive calibration campaign (Gondoin et al 1998a, Gondoin et al 1998b). A comprehensive numerical model of the mirror system (Gondoin et al 1996) was then used to generate an initial calibration database by extrapolating on-ground tests to in-orbit operation conditions and by interpolating between the finite number of measurement points. During the in-orbit calibration programme, appropriate celestial targets were observed to validate this initial database (Gondoin et al 2000). Analysis results indicate that the telescopes' point responses measured in-orbit are identical to on-ground calibration measurements. In particular, extended sources in the center of the telescope field of view can be studied with a ∼5 arcsec spatial resolution (Table 2). Fitting residuals of the spectra of astrophysical plasmas broadly confirm the on-ground calibration of the relative effective area close to the Au M edges. No evidence for contamination is detected close to the C K and O K edges. Measurements of the in-orbit vignetting function match simulation results extrapolated from on-ground calibration. Pointings in the vicinity of the Crab nebula verify the high straylight rejection efficiency of the telescope baffles.

Table 2. In-flight imaging quality of the XMM-Newton X-ray telescopes

Telescope	FWHM (1.5 keV)	HEW	FWHM (8 keV)	HEW
FM2−pn	6.6″	15.1″	6.6″	14.8″
FM3−MOS1	6.0″	13.6″	5.1″	12.5″
FM4−MOS2	4.5″	12.8″	4.2 ″	12.2″

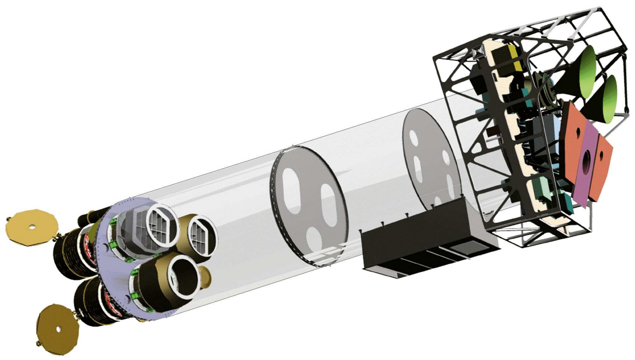

Fig. 1. 'Open' view of the XMM-Newton observatory. To the left the three mirror modules (with the RGA units mounted behind two of them) can be seen, while at the right the back-end of the instrument platform with all the radiators is visible.

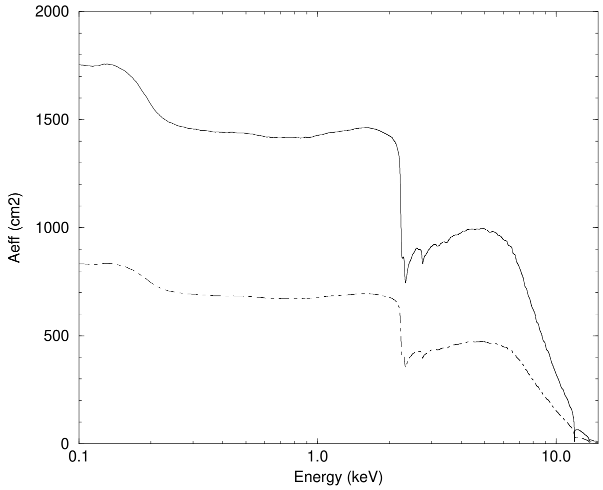

Fig. 2. On-axis effective area of the XMM telescopes without (solid line) and with (dot-dashed line) Reflection Grating Assembly (RGA).

2.2. Attitude Measurement

The spacecraft service module is equipped with redundant star trackers. The design specification was to make an absolute measurement accuracy of 4 arcseconds half-cone angle (95% confidence). The actual resolution of the star tracker centroiding is 1 − 2 arcseconds, therefore after early operations the system has been enabled to report *any* apparent attitude deviations. Preliminary analysis shows that over long periods the spacecraft is stable to within the star tracker measurement noise, except for occasional reported temporary excursions of several arcseconds when a guide star is momentarily lost (Figure 3). As these excursions are recorded, the analysis software (Section 5) automatically corrects for such events.

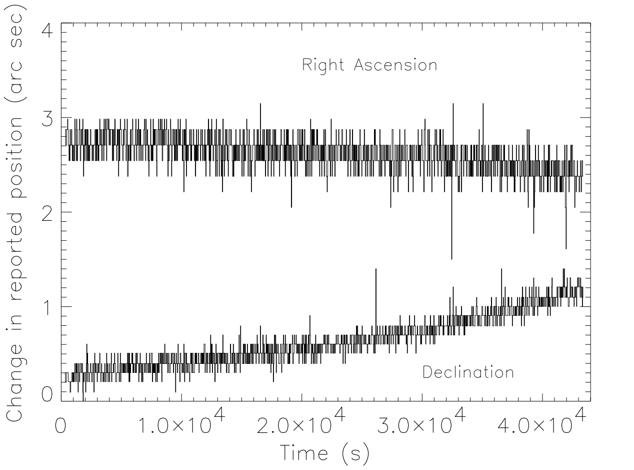

Fig. 3. Specimen reported attitude history data. Relative RA & Dec reported during Revolution 81 observation of Lockman Hole (Right Ascension offset for clarity)

With a compact mirror point spread function, the identification of serendipitous sources of fluxes as low as 10^{-15}ergs cm^{-2}s^{-1} can be statistically limited to $\leq$1 arcsec, so the nominal attitude measurement limits this precision. Detailed trend analysis is under way to establish the systematic effects (tube thermo-elastic deformation, star tracker calibration etc.) which may reduce the 4 arcseconds *absolute* location accuracy, down to the statistical limits. As shown in the paper by Hasinger et al (this issue), knowledge of source locations in the field *already* would allow 1 arcsecond astrometric accuracy.

2.3. Orbit

The orbit of the satellite is highly eccentric, with a $\sim$48 hour period. The perigee is 7000km and apogee of 114000km, while the inclination is $\sim -40^o$. This orbit was chosen to allow the 5 main X-ray cameras to be cooled to between -80^oC – -100^oC using only passive radiators. The lowest portion of this orbit is contained within the radiation belts, so operations are limited to altitudes $\geq$60000km, (Figure 4). Depending on the season, the satellite is located in- or outside the magnetotail even at operational altitudes, and there is a modulation in the particle background fluxes experienced by the instruments. Limited experience to date shows that $\geq$65% of observation time is executed in the lowest background periods.

The configuration of mirrors, optical bench tube, colimators and detector doors prevent a significant damaging proton flux reaching the instruments, even during the highest background periods.

Figure 5 shows the typical background in the PN camera during quiescent periods. Features to note are that for energies below 3 kev the diffuse background (mainly galactic) dominates. At higher energies a flatter hard spectrum results mainly from the un-rejected particle background of Compton, γ-ray and fluorescent X-ray events. In both EPIC cameras there is a fluorescent line feature at Al K (1.487 keV), and in the PN camera a signature of Cu K at 8.048 keV. For reference the plot also shows a spectrum of the brightest source in the Lockman Hole field (few 10^{-14}ergs cm^{-2}s^{-1}). This comparison (both spectra were extracted from a 2 arc minute diameter) shows the power of XMM to perform spectral analysis on fainter sources than heretofore.

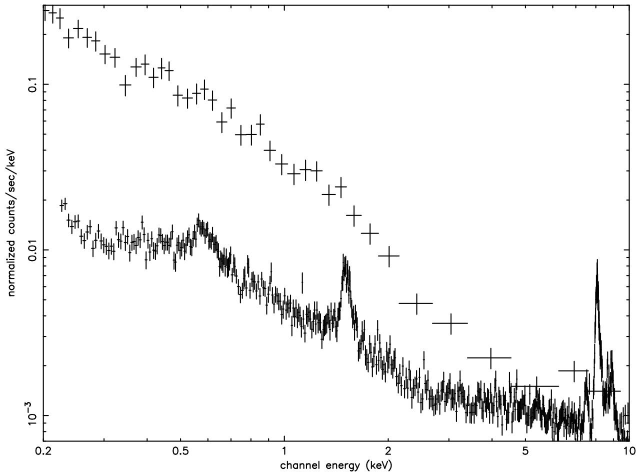

Fig. 5. Comparison of background spectrum in PN camera (lower) for same spatial extraction scale as a typical (10^{-14}ergs cm^{-2}s^{-1} class field source (upper)

3. Ground Station

Normal operations allow coverage of the observational periods of spacecraft orbit with only two ground stations (Perth and Kourou), however there is a seasonally varying gap close to spacecraft apogee of order 1 hour, during which no science operations can be conducted. This implies that uninterrupted exposures of about 65 ks can be implemented at the moment. It is anticipated that by the end of the year 2000 full orbit coverage can be achieved by using an additional operational antenna.

Packets of science data from the 6 instruments, are multiplexed with their housekeeping data and spacecraft telemetry, and transmitted to ground at a rate of 64kbit/s maximum. Spacecraft data are merged with earth reception time references, and transmitted via ground telecommunications links to the Mission Operations Centre at Darmstadt. The MOC monitors real-time payload health, performs commanding of operations, and provides additional analysis of spacecraft data to provide (for example) the *Attitude History Files* for each science observation. The science data are further transmitted to the Science Operations Centre at Villafranca, where science Quick

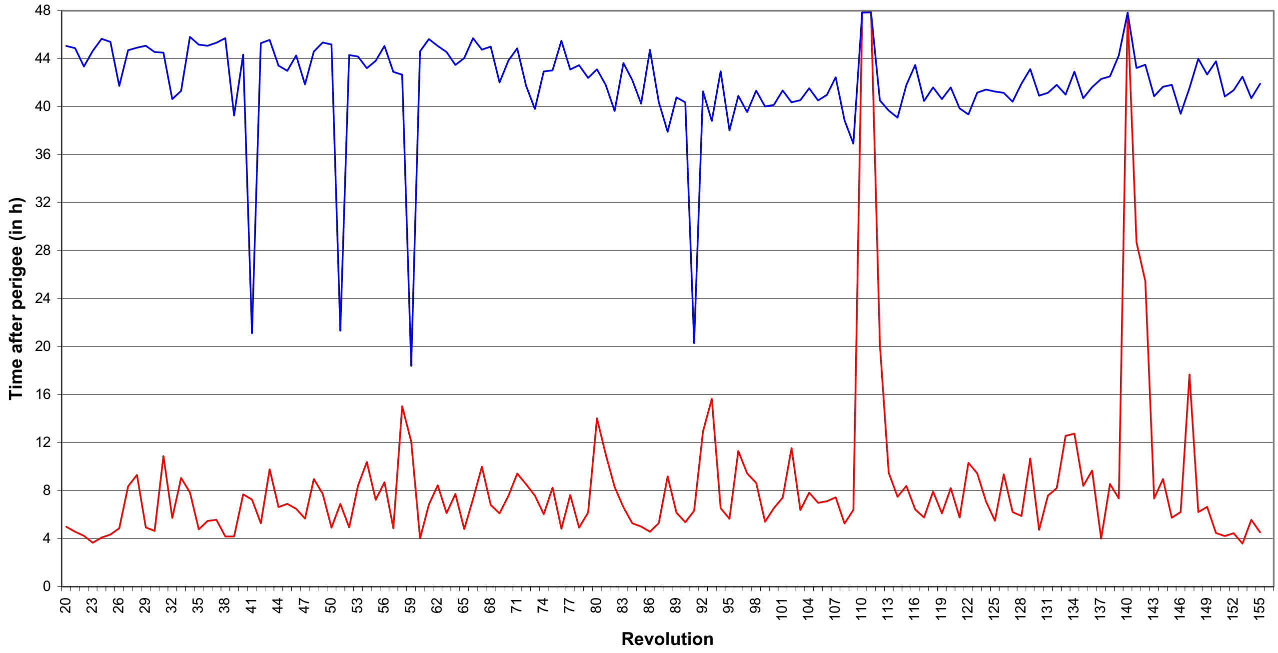

Fig. 4. Time throughout the 48 hour XMM-Newton orbit that the radiation levels are not exceeding critical limits. The red line traces the time after perigee, at which safe operations can begin. The blue line displays the equivalent period *before* perigee. The two large solar flares in summer 2000 can be clearly identified.

Look Analysis is performed. The SOC then processes the data into the *Observation Data Files* (ODF) for transmission to the science community.

4. Science Data Files and Data Flow

The instrument science data, housekeeping and auxillary data necessary to perform analysis are bundled into a data set known as the *Observation Data File* (ODFs). This data set forms the basis of information provided to the Guest Observer community on CD-ROMs. Access to XMM-Newton data can also be achieved via *http : //xmm.vilspa.esa.es/*, where eventually access to all XMM-Newton data will be available.

In order to process the ODFs, such that data are correctly calibrated for further scientific analysis, a data set named the *Current Calibration File* (CCF) is also supplied to the user. These data are offered as the best currently known calibration pertaining to the subject observation. The data not only allow the ODFs to be processed into calibrated datasets, but also provide all the necessary data to reduce the data scientifically (generate response matrices, make photometric corrections etc.). Improved calibration knowledge is provided from the SOC *ftp* site with sets of release notices detailing changes. An indexing mechanism ensures that the latest calibration data set for a particular observation date is always available.

The ODFs are first sent to the Survey Science Centre, where they are pipeline processed to produce a set of standard products (Watson et al, this issue). The Guest Observer receives these pipeline products which include cleaned and calibrated event lists, source detection lists and standard image, spectral and timing products. These form a starting point for the interactive analysis of the datasets. In addition to the standard XMM-Newton observation products, the SSC offers comprehensive catalogued cross-correlation analyses. All these are returned to the XMM-Newton Science Archive, and in the case of US Observers also to the NASA GSFC XMM-Newton Guest Observer Facility.

5. Science Analysis Software

The software used to generate the products has been produced by the SSC and the XMM-Newton SOC, with the extensive support by the instrument hardware teams. It is run in a fixed configuration for the pipeline generation. However the complete set of tasks is bundled together as the *Science Analysis Sub-System* to allow the Guest Observer to perform intercative analysis of the data.

A GUI aids the user to select task parameters and browse data sets, or point to extensive help documentation. Individual tasks have been chained together to make the calibrated lists, form image products, perform complex detection tasks etc.. These *metatasks* can be re-run by the user with different activation parameters or updated calibration files. An interactive data display and filtering tool allows the user to visually inspect the event lists, filter the

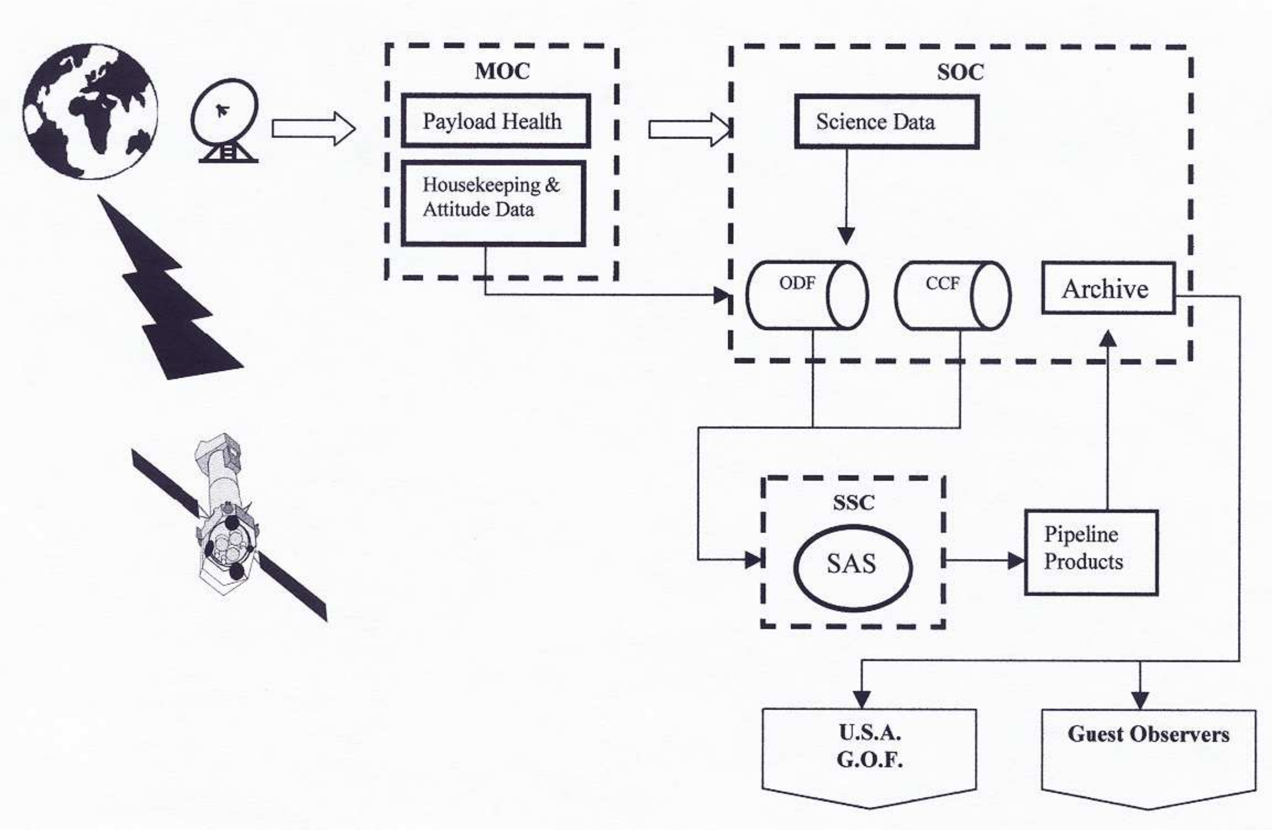

Fig. 6. Summary of the data flow in the XMM Newton ground segment

data with arbitrary selection expressions, extract images and spectra for later analysis with the SAS and other data analysis packages. The SAS contains an interactive calibration viewer which can be used to display each of the corrections applied to the data. This viewer uses the calibration data sets available to the user and links them with the calibration algorithms available in the SAS to display their combined effect.

As noted in the accompanying papers, the proto-type SAS tasks have been used extensively for basic processing. The public release of the collection of software tools will be made before the end of 2000.

6. Calibrations

The SAS has been widely used in analysis of in-flight calibration observations. An overview of the calibration status is supplied in the accompanying instrument descriptions. The data have been gathered to verify the on-ground measurements where the latter were not possible in a flight-representative mode. Due to these extensive ground calibration activities, the existing calibration knowledge was sufficient to enable the scientific analysis as described in the accompanying papers. Nevertheless, verification of the cross-calibration between XMM instruments, and between XMM and other observatories (CHANDRA, Beppo-SAX and RXTE) is on-going.

After public release of the SAS, the calibration and Performance Verification observation data sets will be made public through the XMM-Newton Archive. (See Table 3)

References

Aschenbach B., Citterio O., Ellwood J., et al., 1987 "The High-Throughput Spectroscopic Mission",Report of the Telescope Working Group, Proc.ESA SP-1084

Den Herder J., Brinkmann A., Kahn S. et al., 2001, A&A 365(this issue)

Gondoin Ph., van Katwijk K., Aschenbach B., et al., 1994 SPIE Proc. 2209, 438

Gondoin Ph., Aschenbach B., Brauninger H., et al. 1996, SPIE Proc. 2808, 390

Gondoin Ph., Aschenbach B., Beijersbergen M., et al., 1998a, SPIE Proc. 3444, 278

Gondoin Ph., Aschenbach B., Beijersbergen M., et al., 1998b, SPIE Proc. 3444, 290

Gondoin Ph., Aschenbach B., Erd C., et al., 2000, SPIE Proc., in press.

Hasinger, G., Altieri B., Arnaud M., et al, 2001, A&A 365 (this issue)

Mason K., Breeveld A., Much R., et al., 2001, A&A 365 (this issue)

Revolution No.	Targets Observed	Revolution No.	Targets Observed
47	3C58 on & off axis, NGC2516	76	N132D & Canopus off-axis
48	A496 on & off-axis	77	A S 1101
50	EXO0748-67	78	RXJ 0720.4-3125
51	PKS0537	79	Alph Pic & Canopus off-axis
52	V2416 SGR	81	BPM 16274 & Lockman Hole
53	Capella offaxis	82	Mkn 766 & MS1229.2+6430
54	Capella and Crab off-axis	83	N132D
55	EXO0748-67	84	PKS0558-504 & Mkn421
56	Crab Pulsar & GX13+1	85	PSR0540
57	PKS0312-770 & GX13+1	86	Coma
58	NGC2516 & GX13+1	87	PKS2155-304
59	EXO0748-67	88	Abell 2690 & BPM16274
60	NGC2516 & G21.5-09	89	NGC253 & HZ43
61	Canopus on-axis, GX13+1 off axis & G21.5-09 offset	90	G158-100 & GD153
62	Canopus, GX13+1 and G21.5-09 all off-axis	91	AB Dor & Zeta Puppis
63	MS0737.9+7441	92	LMC X-3 & NGC2516
64	Canopus and G21.5-09 off-axis	93	Coma offset
65	1ES0102-72 and G21.5-09 off-axis	94	3C 273
66	LMC X-3	95	3C 273
67	Canopus off axis and EXO0748-676	96	Akn 564
68	Canopus off axis and CAL 83	97	M87 & IRAS13349+2438
69	YY Gem	98	Coma offset
70	Lockman Hole	99	Coma offset
71	Lockman Hole	100	M31 Core & A 1795
72	AB Dor	101	Coma offset & A 1835
73	Lockman Hole	102	Tycho & OY Car
74	Lockman Hole	104	BPM16274
75	Mkn205		

Table 3. Sumary of Calibration/Performance Verification Observations

Struder L., Briel U., Dennerl K., et al., 2001, A&A 365 (this issue)
Turner, M.J.L., Abbey A., Arnaud M., et al., 2001, A&A 365 (this issue)
Watson, M., Augeres J-L., Ballet B., et al., 2001, A&A 365 (this issue)